INSTITUTE OF PLASMA PHYSICS

NAGOYA UNIVERSITY

RESEARCH REPORT

NAGOYA, JAPAN

Characteristics of Microinstabilities in a Hot Electron Plasma

H. Ikegami, H. Ikezi, T. Kawamura, H. Momota,
K. Takayama and Y. Terashima

IPPJ-73 October 1968

Paper presented at the Third Conference on Plasma Physics and Controlled Nuclear Fusion Research, Novosibirsk, U. S. S. R., August 1968.

Further communication about this report is to be sent to the Research Information Center, Institute of Plasma Physics, Nagoya University, Nagoya, JAPAN.

Abstract

The 150 keV hot-electron plasma is produced in a mirror by pulsed high-power microwaves. Plasma densities of 10^{12} electrons/cm^3 are observed. During the stable afterglow, an instability is triggered artificially by irradiation of a small microwave pulse. The instability is characterized by a sudden disappearance of the hot electrons and the strong burst of microwaves.

The instability is identified to be the electron cyclotron instability both experimentally and theoretically. The rapid plasma loss is also interpreted by the diffusion of particles in velocity space due to the microinstability.

I) Introduction

Hot-electron plasmas[1][2] are generated in a magnetic mirror field (typically 4000G - 1200G - 4000G) and are contained in a stainless steel cavity with a diameter of 30 cm and a length of 40 cm as shown in Fig. 1. The gas used in the experiment is helium at a pressure from 1 to 8 x 10^{-4} Torr. The discharge is produced by a microwave pulse at 6.4 GHz with 20 msec duration and 5 kW power. The microwave power is introducted radially through two opposite pairs of waveguide ports in the cavity wall. The plasmas generated at power levels above 3 kW are very similar in electron temperature and electron density, and consist of hot electrons, cold electrons and ions. The hot electron temperature is determined to be about 150 keV from x-ray spectra. This temperature is observed to be almost constant, or slightly increasing, during the first 140 msec of the quiet afterglow. By measuring the intensity ratio of singlet to triplet helium lines (4713 to 4921Å), the temperature of the cold electrons is found to be 20 eV.

After the removal of the microwave pulse, the plasma density decreases to about one-fifth of the initial value within a few msec and thereafter decays with a longer time constant (30 - 100 msec). The initial rapid decay is due to the loss of low-energy electrons (cold electrons) from the mirror and the successive slower decay suggests that cold electrons are produced during the late afterglow by ionization of the background helium by trapped hot electrons. The hot electron density, immediately after the removal of the microwave power, is about 10^{10} electrons/cm^3 and decays with a time constant of several tens of msec, depending on the background gas pressure.

During the decay period, the ratio of the hot electron density to the cold electron density is about 0.1 to 1 and is constant in time.

In order to determine the radial density profile of the hot electrons produced in the system, the radial emission of x rays from the plasma is observed by scanning with an x-ray telescope along a slit in the cavity wall. The collimation system excludes any reception of unwanted x rays from the cavity wall. The radial distribution of hot-electron density is calculated by using Abel's transformation. The hot electrons are observed to be bunched in a shell structure[1] throughout the microwave discharge and the afterglow of the plasma. The radial density distribution of the cold electrons has the shape of a bell centered on the axis of the machine, while after the power has been removed, the top of the bell is depleted to form a shell. The fact assures that the cold electrons present in the plasma during the afterglow are those produced by ionization of neutral atoms by the hot electrons present in the shell. The decay of this new cold electron distribution is determined now by the longer lifetime (30 - 100 msec) of the hot electrons.

It has been confirmed[1] that the location of the hot-electron shell corresponds to the throat of the single-lobe hyperboloid-like surface of constant magnetic field intensity, which provides the second harmonic resonance for the heating microwave at 6.4 GHz. As the magnetic field is increased, the radius of the throat increases and the radius of the hot-electron shell is observed to follow this growth. In other words, the hot electrons are generated within the mirror always at the zone of constant magnetic field intensity which provides the electron cyclotron frequency at 3.2 GHz.

The heating mechanism is interpreted in terms of stochastic accelerations[3]. Experimentally the rate of heating is found to be $dT/dt \simeq 10$ MeV/sec for 5 kW power, and after 10 msec the hot electrons with $T \simeq 100$ keV attains to about 10^{10} electrons/cm^3 under 10^{-4} Torr.

In the early stage of discharge a large number of cold electrons are produced at the fundamental resonance zone. They couple with the microwave field both in the fundamental and the second harmonic resonance zones. Some of the electrons will preferentially be accelerated within these zones. In the course of multiple reflections, the electrons experience random electric fields. Namely, the initial phase difference between a gyrating electron and the electric field at each traverse of the respective resonance region is assumed to be a random variable. The change in the velocity component perpendicular to the magnetic field is $\langle \Delta v_\perp \rangle = 0$ and $\langle (\Delta v_\perp)^2 \rangle = a^2$, where $\langle\ \rangle$ means the average over the random phase and a is proportional to E, the amplitude of the heating field. The Gaussian distribution of $\exp(-v_\perp^2/Na^2)$ is achieved after N traverses.

The increase in the parallel component of the velocity is $\frac{2}{m}\int \mu \nabla_\parallel B\, v_\parallel\, dt$. Then we have

$$\langle (\Delta v_\parallel)^2 \rangle \simeq \langle (\Delta v_\perp)^2 \rangle \frac{\nabla_\parallel B}{B}\, \ell \ ,$$

where ℓ is the length of the resonance region. Based on these considerations, the heating rate is estimated to be

$$\frac{dT_\perp}{dt} \simeq 2\, t^{-1/3} \quad \text{(MeV/sec)} \ ,$$

for $E \sim 30V/cm$ and $\ell \sim 4$ cm in the second harmonic resonance zone. The degree of anisotropy in temperature is found to be $T_\perp/T_\parallel \sim 10$. The stochastic heating is expected to be more effective in the second harmonic resonance zone than in the fundamental resonance zone, because of the wider interaction area. This fact reasonably explains the formation of the hot-electron shell.

II) Instability

Several methods[4][5] have been reported for triggering instabilities articially. In the present device, the instability can be triggered[2] by introducing an additional small microwave pulse of about 100 W at the same frequency as the heating microwave pulse from 1 - 50 msec after the end of the main pulse. For some conditions at pressures lower than the critical value of 10^{-4} Torr, the plasma is spontaneously unstable. However, no physical difference is observed between the triggered instability and the spontaneous one. When the pressure is above 8×10^{-4} Torr, no instability could be triggered.

Some details of the triggered instability are shown in Fig. 2. The instability is characterized by the sudden loss of hot electrons from the mirror bottle and by the strong burst of microwave emission. The signals related to the hot electrons, like x-ray signal, microwave noise, scintillator output and diamagnetic signals, disappear within several μsec. However, those related to the cold electrons, like Langmuir probe signal, light intensity and plasma density, decay at a slower time constant of about 200 μsec.

At the onset of the instability, a burst of energetic electrons

escaping from the magnetic mirror is observed along the axis of the machine. These electrons are detected by a plastic scintillator through twelve different thicknesses of aluminum foil, working as an energy selector. The energy spectrum of these electrons is found to have an average energy of 200 keV and a high energy tail up to 500 keV. Since the temperature of these electrons (200keV) is not very much different from the temperature of the x-ray bremsstrahlung (150 keV), it is reasonable to assume that the electrons detected by the scintillator, belong to the same group of electrons which lose their energy by x-ray bremsstrahlung.

The instability is further accompanied by a fast rising x-ray signal, probably coming from the hot electrons impinging on the cavity walls. A pair of scintillator probes is used for checking the possible correlation between the signals originated by the instability. The scintillator probes are 10 cm apart on the same field line. No correlation is observed[2] between the signals to these probes. Taking into consideration the axial loss accompanied by the instability, this absence of correlation implies that the instability is not a type of macroscopic flute instability.

The strong microwave burst accompanied by the instability characterizes the nature of the instability. The microwave emission is composed of harmonics of 2.1 GHz for the typical mirror field (4000G - 1200G - 4000G). The lower-frequency harmonics (2.1, 4.2 and 6.3 GHz) are collected by a loop antenna, while the higher-frequency emissions (8.4, 10.5, 12.6 and the frequency region up to 18.9 GHz) are collected by x-band waveguides. For the mirror field (8000G - 2400G - 8000G), the frequency of the microwave radiation associated with the instability is observed to be 4.2 GHz. In this case both

hot and cold electrons are accumulated at the center of the machine. The relation between the fundamental frequency of the microwave burst and the electron cyclotron frequency is given experimentally by $f = 0.66\ f_{ce}$.

Although the magnetic field is varied around the optimum field intensity (4000G - 1200G - 4000G), the variation of the microwave frequency (2.1 GHz) with the magnetic field at the mirror center is insensitive. This is quite reasonable, since the hot electrons are produced in a shell which touches the throat of the single-lobe hyperboloid-like surface of the constant magnetic field intensity, which provides the electron cyclotron frequency at 3.2 GHz. Since the frequency 6.4 GHz of the heating microwaves is fixed, the magnetic field intensity which gives rise to the second harmonic resonance is also fixed. This fact implies that most hot electrons stay always around the region of 1140G, corresponding to the second harmonic resonance, as far as the mirror remains around the optimum field intensity. When the field is changed to give the production and heating at the center of the mirror at the fundamental cyclotron resonance, the frequency of the microwave radiation is doubled and becomes 4.2 GHz.

The power of the microwave burst, associated with the harmonics, decreases for higher harmonic numbers. The ratio for two successive harmonics is found to be 10 dB. The main contribution to the total power emission comes from the fundamental component and the power collected by the probe is found to be several 10 W within a bandwidth of 5 MHz. The amplitude of the burst increases with the growth rate of about 0.1 μsec, and reaches its maximum at about 1 μsec after the initiation of the instability.

Furthermore the radiation is detected by using a pair of loop antenna inserted into the cavity; one is fixed and the other is movable along the axis of the machine. The microwave emission accompanied with the instability is found to be standing electromagnetic waves with the wavelength of 19 cm for 2.1 GHz. The mode of the wave is determined by the diameter of the cylindrical side arms to be TE_{11} mode of circular waveguide. By rotating one loop antenna with respect to the other, phase correlation is measured. The waves are found to be composed of circularly polarized transverse electric fields propagating in the whistler mode. When the magnetic field direction is reversed, the standing wave is observed to rotate in the opposite sense. To our best knowledge, the instability, characterized by the frequency lower than the cyclotron frequency and by the right-hand transverse waves, cannot be other than the electron cyclotron instability[6][7][8].

In order to confirm the identification, the instability is further analysed theoretically by taking into account the actual experimental conditions, i.e. the inhomogeneity in both magnetic field and plasma densities. In view of the experimental results, the unperturbed velocity distribution of the electrons is supposed to be

$$F_0 (\vec{r} , \vec{v}) = n_c(z)\ \delta(\vec{v}) + n_h(z)\ f_h(z , \vec{v}) \quad . \qquad (1)$$

The distribution function for the hot electrons is chosen to be a loss-cone distribution, which in the midplane coincides with bi-maxwellian distribution with the temperatures $T_\perp$ and $T_\parallel$. The suffices $\perp$ and $\parallel$ are with respect to the magnetic field. The unperturbed distribution function for the hot electrons is

$$f_h(z,\vec{v}) = \begin{cases} \text{const. } \exp\left\{-\frac{m}{2T_{\parallel}}\left(v_{\parallel}^2 + \frac{B(z)-B_0}{B(z)} v_{\perp}^2\right) - \frac{m}{2T_{\perp}} \frac{B_0}{B(z)} v_{\perp}^2\right\} \\ \qquad \text{for } \frac{Bm-B(z)}{B(z)} v_{\perp}^2 - v_{\parallel}^2 \geq 0 \ , \\ 0 \qquad \text{for } \frac{Bm-B(z)}{B(z)} v_{\perp}^2 - v_{\parallel}^2 < 0 \ , \end{cases} \tag{2}$$

where z is the distance from the midplane and the magnetic field $B(z)$ is, for simplicity, assumed to be

$$B(z) = \frac{Bm+B_0}{2} - \frac{Bm-B_0}{2} \cos\left(\frac{\pi}{L} z\right) \ . \tag{3}$$

Starting with the Vlasov equation, we seek the perturbed electric field to the form

$$E(z,t) \propto \exp\left\{i \int^z k(z)dz - i\omega t\right\} \ , \tag{4}$$

with $k = k_r + ik_i$ and $\omega = \omega_r + i\omega_i$. Under the boundary condition that the electric field has the same amplitude at $z = \pm L$, the solution of the dispersion equation is found to be

$$k_r^2(z) = \frac{\omega_r^2}{c^2}\left\{1 + \frac{\omega_p^2}{\omega_r(\omega_c - \omega_r)}\right\} \ , \tag{5}$$

and

$$\omega_i = \int \gamma \left(\frac{\partial \omega_r}{\partial k_r}\right)^{-1} dz \Big/ \int \left(\frac{\partial \omega_r}{\partial k_r}\right)^{-1} dz \ , \tag{6}$$

where the plasma frequency ω_p and the cyclotron frequency ω_c are functions of z, and $\gamma(\omega_r,z)$ is given by

$$\gamma(\omega_r,z) = \frac{\pi}{2}\frac{n_h}{n_c+n_h}\omega_p{}^2\left(\omega_r+\frac{\omega_p^2}{2}\frac{\omega_c}{(\omega_c-\omega_r)^2}\right)^{-1}$$

$$\times\left[\frac{1}{2}\frac{\partial}{\partial v_\parallel}\int_0^\infty v_\perp^2\, f_h 2\pi v_\perp dv_\perp - \frac{\omega_c}{k}\int_0^\infty f_n 2\pi v_\perp dv_\perp\right]_{v_\parallel = \frac{\omega_r-\omega_c^*}{k}}, \tag{7}$$

where ω_c^* is the relativistic electron cyclotron frequency.

A typical example of numerical computations is shown in Fig. 3, where ω_i is plotted against ω_r. The result is based on the following assignments of the parameters: $B_0 = 1.26$ kG, $B_m = 4.24$ kG, the fraction of the hot electron component is 0.03, $n_h + n_c = 2 \times 10^{11}$/cc, and $T_\perp/T_\parallel = 15$.

In Fig. 3 it is shown that the growth rate is maximum at 2.1 GHz, which is just what has been observed in the experiment. The agreement in frequency is quite satisfactory, but there still remains discrepancy in wavelength.

III) Discussion of Enhanced Loss

It is quite reasonable to assume that the strong microwave field is the driving force of the rapid particle decay. The hot electrons lose their transverse energies by exciting the instability and fall into the loss cone. Theoretical analysis predicts that by the development of instability a considerable fraction of the hot electrons will be lost in the direction along the magnetic field, as well as in the

radial direction. In fact the particle loss along the magnetic field is estimated to be at most 40 percent of the hot electrons based on a quasi-linear theory.

To avoid unnecessary complexity, the magnetic field is assumed to be uniform. The formulation is non-relativistic and only the hot electron component is considered. By usual procedure, the change in time of the electron distribution is expressed as

$$\frac{\partial}{\partial t} F_0(v_\perp, v_\parallel, t) = \left[\left(\frac{\omega_c}{k} \frac{1}{v_\perp} \frac{\partial}{\partial v_\perp} + \frac{\partial}{\partial v_\parallel} \right) D \right.$$

$$\left. \times \left(\frac{\omega_c}{k} \frac{1}{v_\perp} \frac{\partial}{\partial v_\perp} + \frac{\partial}{\partial v_\parallel} \right) F_0(v_\perp, v_\parallel, t) \right]_{k=k(v_\parallel)} , \qquad (8)$$

where $k(v_\parallel)$ satisfies the resonant condition $\omega_r - \omega_c = k v_\parallel$, and D relates with the perturbed electric field $E_k(t)$ as

$$D = 8\pi L \left(\frac{e}{m}\right)^2 \frac{v_\perp^2}{|v_\parallel|} \frac{k^2}{\omega_r^2} |E_k(t)|^2 . \qquad (9)$$

By change of the variables

$$\xi \equiv \frac{1}{2} v_\perp^2 - \int \frac{\omega_c}{k(v_\parallel)} dv_\parallel , \qquad \eta \equiv v_\parallel , \qquad (10)$$

Eq. (8) is rewritten as

$$\frac{\partial}{\partial t} F_0(\xi, \eta, t) = \frac{\partial}{\partial \eta} D \frac{\partial}{\partial \eta} F_0 \quad (\xi, \eta, t) . \qquad (11)$$

This equation implies that in velocity space the resonant electrons

diffuse along the lines of ξ = constant, which are hereafter called "diffusion lines".

Now we shall discuss the case of the magnetic mirror field given in Eq. (3). Let us define .

$$\varepsilon = \frac{m}{2}(v_{\parallel}^2+v_{\perp}^2) \quad \text{and} \quad \mu = \frac{m}{2} v_{\perp}^2/B(z) \quad . \tag{12}$$

The diffusion lines in $\varepsilon = \mu$ space (Fig. 4) are now

$$\varepsilon - \frac{\omega_r}{\omega_c(z)} B(z)\mu = \text{const.}, \tag{13}$$

where ω_r is the frequency of the most unstable mode discussed in the previous section. Let the resonant velocity for this mode be $v_r(z) = \{\omega_r - \omega_c\}/k(z)$, then the resonant zone in $\xi - \mu$ space is covered by the lines,

$$\varepsilon = B(z)\mu + \frac{m}{2} v_r^2(z) \quad . \tag{14}$$

From the dispersion relation one will see that $v_r^2(z)$ is increasing with $B(z)$, so that the resonance zone is defined by

$$B_m\mu + \frac{m}{2} v_r^2(L) > \varepsilon > B_0\mu + \frac{m}{2} v_r^2(0) \quad . \tag{15}$$

Note that the loss cone is defined by $\varepsilon > \mu B_m$ and the electrons initially distribute over the region of $\mu B_m \geq \varepsilon \geq \mu B_0$.

By development of the instability, the electrons which satisfy the resonant condition, Eq. (15), will continuously diffuse along the diffusion lines defined by Eq. (13), since there exists a diffusion

line at any point on the resonance zone. In consequence they fall into the loss cone. The situation is expressed by

$$F_0(\varepsilon,\mu,z,t\to\infty) = \begin{cases} F_0(\varepsilon,\mu,z,t=0) & \text{for} \quad B_0\mu + \frac{m}{2} v_r^2(0) > \varepsilon \\ 0 & \text{for} \quad B_0\mu + \frac{m}{2} v_r^2(0) < \varepsilon \end{cases} \tag{16}$$

For the distribution given in Eq. (2), these considerations lead the particle loss of at most 40 percent of the initial density along the magnetic field.

Experimentally enhanced particle losses are observed both in axial and radial directions when the instability is triggered. Being accompanied with the strong microwave burst, almost all the hot electrons are lost. Furthermore it has been observed that more electrons escape from the region closer to the mirror point than from the central region. This is also predicted by the theory. After the hot electrons have been driven off within several μsec, cold electrons are not generated anymore. The cold-electron density is observed to decay at a larger time constant of about 200 μsec. The fact clearly indicates that the instability is of hot-electron nature.

Acknowledgements

We express our appreciation to Mr. M. Hosokawa for his assistance throughout the experiments and to Professor S. Tanaka, of Kyoto University, Kyoto, for his interests. The authors wish to acknowledge the continued interest and encouragement of Professor K. Husimi throughout this work.

References

(1) H. Ikegami, H. Ikezi, M. Hosokawa, S. Tanaka and K. Takayama, Phys. Rev. Letters 19, 778 (1967)

(2) H. Ikegami, H. Ikezi, M. Hosokawa, K. Takayama and S. Tanaka, Phys. Fluids 11, 1061 (1968)

(3) D. E. Hall and P. A. Sturrock, Phys. Fluids 10, 2620 (1967)

(4) W. A. Perkins and R. F. Post, Phys. Fluids 6, 1537 (1963)

(5) W. A. Perkins and W. L. Barr, Plasma Physics and Controlled Nuclear Fusion Research (International Atomic Energy Agency, Vienna, 1966), Vol. II, p. 115

(6) R. N. Sudan, Phys. Fluids 8, 153 (1965)

(7) J. E. Scharer, Phys. Fluids 10, 652 (1967)

(8) There have been several papers related to the instability in hot-electron plasmas, for examples, V. V. Alikaev, V. M. Glagolev and S. A. Morozov, "Anisotropic Instability of a Hot Electron Plasma Confined in Adiabatic Trap", Abstract of 2nd European Conference on Controlled Fusion and Plasma Physics (Stockholm, 1967), and W. A. Perkins and W. L. Barr, Phys. Fluids 11, 388 (1968).

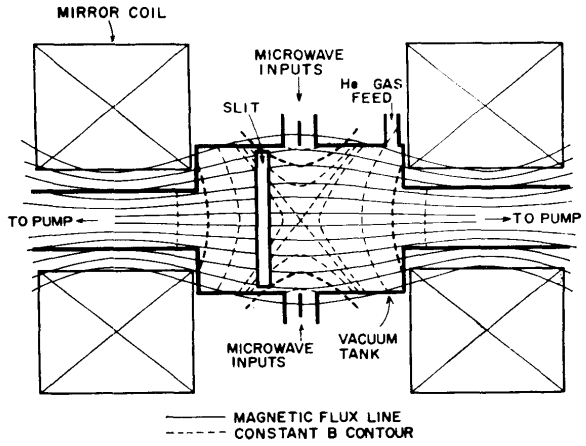

Fig. 1. Schematic diagram of the hot electron plasma device, named TPM after <<test plasma by microwave>>. The bold hyperbola-like lines vertically crossing the flux lines indicate the fundamental cyclotron resonance region. The other bold hyperbola-like lines at the top and the bottom of the cavity denote the second harmonic cyclotron resonance region.

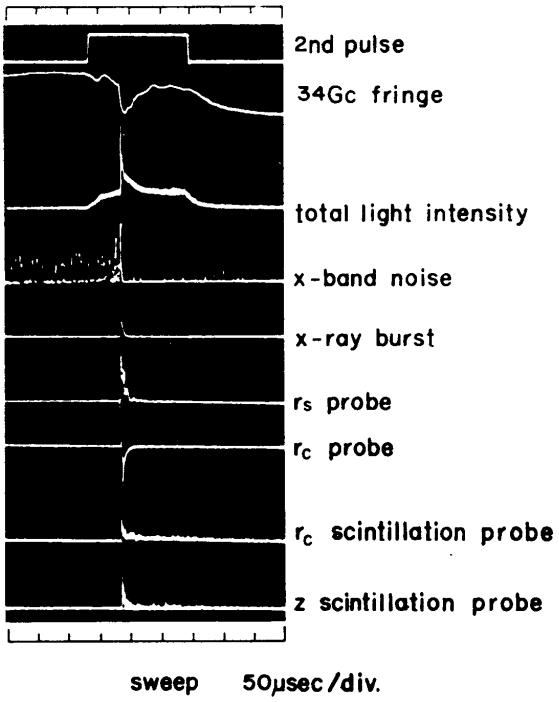

Fig. 2. Signals accompanied with the instability triggered by the second microwave pulse (50 W). The onset of the instability is seen about 70 μsec after the pulse front. Helium (2 x 10^{-4} Torr) is admitted in steady flow operation. In the 6th and 7th traces, r_s denotes a radially inserted Langmuir probe situated close to one end-walls of the cavity and r_c that at the center of the cylindrical cavity wall. Both probes are 10 cm apart on the same magnetic lines of force.

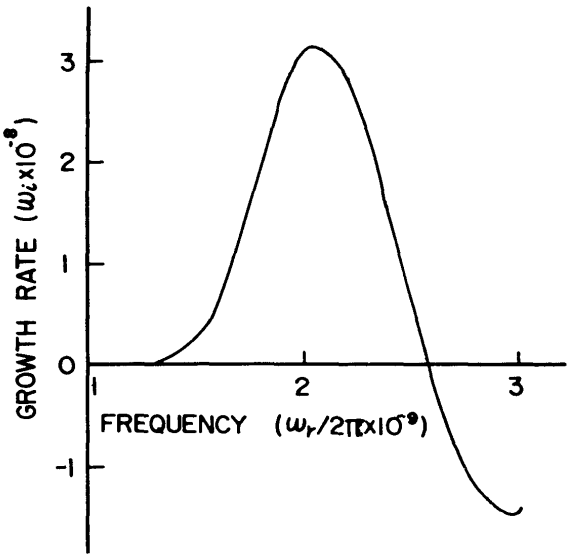

Fig. 3. Growth rate ω_i as a function of frequency $\omega_r/2\pi$. The growth rate attains its maximum at 2.1 GHz. Since the inhomogeneity in magnetic field, as well as in spatial density distribution, is fully taken into account, simple relation between k and ω_r cannot be displayed in a familiar fashion.

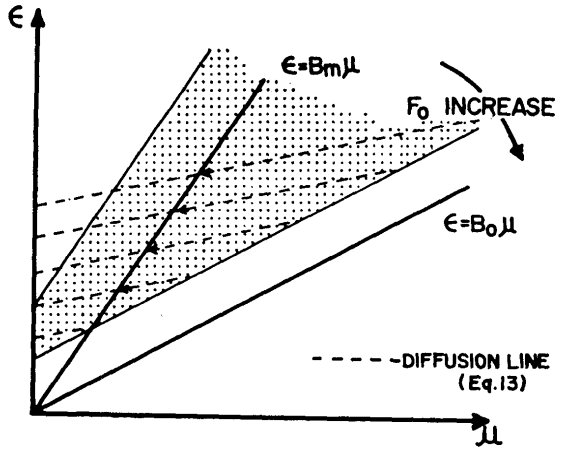

Fig. 4 Diffusion of particles in $\varepsilon - \mu$ space. Dotted region indicates the resonance zone, Eq. (15). Particles are initially in the region between $\varepsilon = \mu B_0$ and $\varepsilon = \mu B_m$. Resonant particles diffuse along the diffusion lines and be lost into the loss cone. Nearly 40% of the total hot-electrons are lost in this mechanism.